

1 **A NOVEL PREGNANT RAT MODEL FOR LABOR INDUCTION AND**
2 **AUGMENTATION WITH OXYTOCIN**

3

4 Tusar GIRI, MD, PhD

5 Department of Anesthesiology, Washington University School of Medicine, St. Louis, MO

6

7 Jia JIANG, MD¹

8 Department of Anesthesiology, Washington University School of Medicine, St. Louis, MO

9

10 Zhiqiang XU, PhD²

11 Department of Anesthesiology, Washington University School of Medicine, St. Louis, MO

12

13 Mr. Ronald MCCARTHY, BA

14 Department of Obstetrics and Gynecology, Washington University School of Medicine, St.
15 Louis, MO

16

17 Carmen M. HALABI, MD, PhD

18 Department of Pediatrics, Washington University School of Medicine, St. Louis, MO

19

20 Eric TYCKSEN, PhD

21 Department of Genetics, Washington University School of Medicine, St. Louis, MO

22 Alison G. CAHILL, MD, MSCI³

23 Department of Obstetrics and Gynecology, Washington University School of Medicine, St.

24 Louis, MO

25

26 Sarah K. ENGLAND, PhD

27 Department of Obstetrics and Gynecology, Washington University School of Medicine, St.

28 Louis, MO

29

30 Arvind PALANISAMY, MD, FRCA*

31 Department of Anesthesiology

32 Department of Obstetrics and Gynecology

33 Washington University School of Medicine, St. Louis, MO

34

35 **Present Address**

36 ¹Department of Anesthesiology, Beijing Chaoyang Hospital, Capital Medical University,

37 Beijing, China

38

39 ²Department of Radiation Oncology, Washington University School of Medicine, St. Louis, MO,

40 63110, USA.

41

42 ³Department of Women's Health, The University of Texas at Austin, Dell Medical School,

43 Texas, USA.

44 **Conflict of Interest**

45 The authors report no conflict of interest.

46

47 **Funding Sources**

48 Arvind Palanisamy was supported by departmental start-up funds.

49 Sarah K. England was supported by grants from the National Institute of Child Health and
50 Human Development (R01 HD088097 and R01 HD096737).

51 Carmen M. Halabi was supported by NIH grant K08 HL135400.

52 RNA-seq experiments conducted at the Genome Technology Access Center (GTAC) were
53 partially supported by the National Cancer Institute Cancer Center Support grant P30 CA91842
54 to the Siteman Cancer Center; by the Institute of Clinical and Translational Sciences/Clinical and
55 Translational Sciences Award grant UL1TR002345 from the National Center for Research
56 Resources, a component of the NIH; and by the NIH Roadmap for Medical Research.

57

58 The funding sources had no role in the design, collection or interpretation of data, and the
59 decision to submit for publication.

60

61 **Paper presentation information:** This abstract was presented for Oral Presentation at the 50th
62 Annual Meeting of the Society for Obstetric Anesthesia and Perinatology, Miami, FL, May 9-13,
63 2018.

64

65 ***Corresponding author**

66 Arvind Palanisamy, MD, FRCA

67 Department of Anesthesiology

68 Department of Obstetrics and Gynecology

69 Washington University School of Medicine, St. Louis, MO, 63110

70 Tel: 314-362-2628

71 Email: arvind.palanisamy@wustl.edu

72

73 **Word count:** 3425

74

75

76

77

78

79

80

81

82

83

84

85

86

87 **ABSTRACT**

88

89 **Background:** Despite the widespread use of oxytocin for induction of labor, mechanistic
90 insights into maternal and neonatal wellbeing are lacking because of the absence of an animal
91 model that recapitulates modern obstetric practice.

92

93 **Objective:** The objectives of this research were to create and validate a hi-fidelity animal model
94 that mirrors labor induction with oxytocin in parturients and to assess its translational utility.

95

96 **Study Design:** The study was performed in timed-pregnant Sprague Dawley dams. The model
97 consisted of a subcutaneously implanted microprocessor-controlled infusion pump on gestational
98 day 18 that was pre-programmed to deliver an escalating dose of intravenous oxytocin on
99 gestational day 21 to induce birth. Once predictable delivery of healthy pups was achieved, we
100 validated the model with molecular biological experiments on the uterine myometrium and
101 telemetry-supported assessment of changes in intrauterine pressure. Finally, we applied this
102 model to test the hypothesis that labor induction with oxytocin was associated with oxidative
103 stress in the newborn brain with a comprehensive array of biomarker assays and oxidative stress
104 gene expression studies.

105

106 **Results:** During the iterative model development phase, we confirmed the optimal gestational
107 age for pump implantation, the concentration of oxytocin, and the rate of oxytocin
108 administration. Exposure to anesthesia and surgery during pump implantation was not associated
109 with significant changes in the cortical transcriptome. Activation of pump with oxytocin on

110 gestational day 21 resulted in predictable delivery of pups within 8-12 hours. Increased
111 frequency of change of oxytocin infusion rate was associated with dystocic labor. Labor
112 induction and augmentation with oxytocin was associated with increased expression of the
113 oxytocin receptor gene in the uterine myometrium, decreased expression of the oxytocin receptor
114 protein on the myometrial cell membrane, and cyclical increases in intrauterine pressure.
115 Examination of the frontal cortex of vaginally delivered newborn pups born after oxytocin-
116 induced labor did not reveal an increase in oxidative stress compared to saline-treated control
117 pups. Specifically, there were no significant changes in oxidative stress biomarkers involving
118 both the oxidative stress (reactive oxygen/nitrogen species, 4-hydroxynonenal, protein carbonyl)
119 and the antioxidant response (total glutathione, total antioxidant capacity). In addition, there
120 were no significant differences in the expression of 16 genes emblematic of the oxidative stress
121 response pathway.

122

123 **Conclusions:** Collectively, we provide a viable and realistic animal model for labor induction
124 and augmentation with oxytocin. We demonstrate its utility in addressing clinically relevant
125 questions in obstetric practice that could not be mechanistically ascertained otherwise. Based on
126 our findings, labor induction with oxytocin is not likely to cause oxidative stress in the fetal
127 brain. Adoption of our model by other researchers would enable new lines of investigation
128 related to the impact of perinatal oxytocin exposure on the mother-infant dyad.

129

130 **Keywords:** pregnant rat; animal model; oxytocin; labor induction; uterine myometrium; fetal
131 brain; oxidative stress; intrauterine telemetry; oxytocin receptor; RNA-sequencing.

132

133 **INTRODUCTION**

134

135 Labor induction and augmentation with oxytocin (Oxt) is one of the most prevalent clinical
136 interventions in modern obstetric practice(1-5). Despite widespread use for over 50 years, most
137 research has focused on the contractile effects of Oxt and associated obstetric outcomes(4-7).
138 Whether Oxt affects the fetus remains sparsely studied, despite controversial epidemiological
139 evidence suggesting a link between the use of Oxt and neurodevelopmental disorders (8-14).
140 Importantly, most preclinical studies that examine this question do so without inducing birth(15-
141 18), making them contextually less germane. An important scientific roadblock is the absence of
142 an animal model that mirrors induction of labor in pregnant women with Oxt, presumably due to
143 the technical difficulty in delivering an incrementally higher dose of intravenous Oxt over time
144 in a free-moving animal. In this report, we surmounted these challenges to create and validate a
145 hi-fidelity pregnant rat model for elective labor induction and augmentation with Oxt using an
146 implantable, programmable, microprocessor-controlled precision drug delivery pump.

147

148 **MATERIALS AND METHODS**

149

150 **Study design**

151 All experiments reported here were approved by the Institutional Animal Care and Use
152 Committee at Washington University in St. Louis (#20170010) and comply with the ARRIVE
153 guidelines. A schematic of the study design is presented in **Fig. 1**.

154

155

156 **Development of the pregnant rat model for labor induction and augmentation with Oxt**

157 The system consists of a subcutaneously placed iPRECIO[®] infrared-controlled microinfusion
158 pump (SMP-200, Primetech Corporation) connected to the right internal jugular vein in an
159 embryonic day (E)18 Sprague Dawley dam (Charles River Laboratories) (presented as a photo
160 montage in **Fig. 2**). Briefly, the dam was anesthetized with 2% isoflurane followed by
161 subcutaneous implantation of the iPRECIO[®] pump approximately 2-3 cm below the nape of the
162 neck and creation of a tunnel to deliver the pump tubing next to the internal jugular vein, into
163 which it was secured in place with ligatures. The reservoir of the iPRECIO[®] pump was primed
164 with sterile normal saline prior to implantation and was pre-programmed to deliver an infusion
165 rate of 10 μ l/h for 72 h to keep the tubing patent until E21. Two hours before completion of the
166 saline infusion at 72 h, the reservoir was accessed subcutaneously under brief isoflurane
167 anesthesia to aspirate the saline and was refilled with 900 μ l of Oxt (Selleck Chemicals, 50
168 μ g/mL in normal saline). This was followed by the pre-programmed infusion rate of 5 μ l/h for 4
169 h, 10 μ l/h for 4 h, 20 μ l/h for 4 h, and 30 μ l/h for 12 h (iPRECIO[®] Management System) (**Fig. 3**).

170

171 **Validation experiments**

172 Though the witnessed birth of pups offered functional validation, we examined the effect of Oxt
173 on the uterine myometrium with molecular biological assays, immunohistochemistry, and
174 telemetric assessment of changes in uterine pressure.

175

176 **(i) *OxtR* gene expression:** Briefly, approximately 0.5 cm x 1 cm rectangular piece of myometrial
177 tissue was harvested from the anti-mesometrial aspect of the uterus after 8-12 h of exposure to

178 either Oxt (100 mcg/mL concentration) or saline. Sample processing and OxtR qPCR was
179 performed with a custom TaqMan[®] OxtR probe as described by us previously(19).

180

181 **(ii) Western blot for OxtR expression:** Membrane-associated proteins were isolated from
182 approximately 100 mg of uterine myometrial tissue using Mem-PER Plus Membrane Protein
183 Extraction Kit (catalog# 89842, ThermoFisher Scientific, Inc.) following manufacturer's
184 instructions and subjected to immunoblotting with appropriate positive and negative controls
185 (Cat#: LY400333, Origene Technologies, Inc). Details are provided in the Supplementary
186 Materials and Methods.

187

188 **(iii) Immunohistochemistry:** Briefly, 5- μ m frozen sections of uterine myometrium embedded in
189 OCT compound were obtained using Leica CM1510 S cryostat and immunostained for
190 phosphorylated myosin light chain kinase (1:200 rabbit anti-mouse phosphomyosin light chain
191 kinase, Invitrogen) and imaged with the Zeiss Axioskop 40 microscope. OxtR protein expression
192 was assessed by immunostaining with goat anti-rat OXTR antibody (1:100; Origene) and
193 revealed with Alexa Fluor[®] 594 labeled rabbit anti-goat antibody (1:300, Invitrogen). All
194 primary antibodies were incubated overnight at 4°C followed by a 1 h incubation with secondary
195 antibodies at room temperature. Imaging was performed with Olympus BX60 fluorescence
196 microscope with designated filter sets.

197

198 **(iv) Uterine telemetry:** To assess whether initiation of Oxt was temporally associated with
199 increase in intrauterine pressure, we performed pressure recordings with telemetry as described

200 previously by us for mice (20, 21). Briefly, under isoflurane anesthesia and sterile precautions,
201 we inserted a pressure catheter in the right horn between the uterine wall and the fetus under
202 sterile precautions during pump implantation in E18 dams. To minimize the possibility that
203 telemetry recordings could represent spontaneous labor, we advanced the time of replacement of
204 saline with Oxt to 48 h instead of 72 h (i.e., E20 - two days before term gestation). The pressure
205 catheter was connected to a PhysioTel PA-C10 transmitter (Data Sciences International) placed
206 in the lower portion of the abdominal cavity. Telemetry recordings were performed at 500 Hz
207 with Dataquest ART data acquisition system version 4.10 (DSI) sampling every 5 min for 15 sec
208 intervals for 6 h at baseline, followed by recordings 48 h later when Oxt was initiated and
209 continued until the birth of the pups.

210

211 **Effect of *in utero* exposure to anesthesia and surgery on the neonatal cortical transcriptome**

212 To rule out the possibility of adverse effects on the fetal brain from intrauterine exposure to
213 anesthesia and surgery during pump implantation(22, 23), we examined the cortical
214 transcriptome of newborn pups delivered spontaneously by unhandled *vs.* surgically implanted
215 dams. Briefly, 2 brains from spontaneously delivered newborn pups of either sex were collected
216 within 2 h of birth from 6 dams (n=3 each for spontaneous labor and saline-filled iPRECIO[®]
217 pump at E18). Total RNA was extracted from the right cerebral cortex using RNAeasy kit
218 (Qiagen) and subjected to RNA-seq (Genome Technology Access Center core facility). Only
219 RNA with RIN > 9.5 were used for RNA-seq. Processing of samples, sequencing, and analysis
220 were done as described by us previously (19) and in the Supplementary Materials and Methods.

221

222 **Assessment of biomarkers of oxidative stress in the newborn brain**

223 Oxt-induced cyclical uterine contractions cause lipid peroxidative injury(24), decrease the anti-
224 oxidant glutathione in cord blood(25), and increase amniotic fluid lactate(26, 27) suggesting the
225 possibility of oxidative stress. Because the developing fetal/neonatal brain is vulnerable to
226 oxidative stress (28), we used our model to investigate this question. Briefly, brains were isolated
227 from vaginally delivered newborn pups immediately after birth, snap frozen, and stored at -80°C
228 for oxidative stress assays. Cortical lysates were prepared according to the assay type and protein
229 concentration was determined using BCA Protein Assay Kit (ThermoFisher Scientific) prior to
230 the assays. All assays were performed in duplicate, and fluorescence/absorbance was read with
231 Tecan Infinite[®] M200 PRO multimode plate reader using appropriate filter sets as recommended
232 by the manufacturer. We assayed for total free radicals (OxiSelect[™] In Vitro ROS/RNS Assay
233 Kit, #STA-347), 4-hydroxynonenal (lipid peroxidation marker, OxiSelect[™] HNE Adduct
234 Competitive ELISA Kit, # STA-838), protein carbonyl (marker of oxidative damage to proteins;
235 OxiSelect[™] Protein Carbonyl ELISA kit, # STA-310), total glutathione (OxiSelect[™] Total
236 Glutathione Assay kit, # STA-312), and total antioxidant capacity (OxiSelect[™] TAC Assay Kit,
237 # STA-360). All assays were purchased from Cell BioLabs, Inc (San Diego, CA).

238

239 **Expression of genes mediating oxidative stress in the newborn brain**

240 From the same set of experiments as above, brains were isolated from additional pups born after
241 exposure to either Oxt or saline (n= 6-8 per group), snap frozen, and immediately stored at -
242 80°C. Processing of total RNA for gene expression experiments was performed as described by
243 us previously(19). Expression levels of 16 genes relevant to oxidative stress (*Mtnd2*, *Mtnd5*,
244 *Mtcyb*, *Mt-co1*, *Mt-atp8*) and antioxidant (*Sod1*, *Sod2*, *Gpx1*, *Gpx4*, *Prdx1*, *Cat*, *Gsr*, *Nox3*,

245 *Nox4*, *Txnip*, *Txrd2*) pathways were assayed in duplicate along with four endogenous
246 housekeeping control genes (*18S rRNA*, *Gapdh*, *Pgk1*, and *Actb*) and reported as described
247 previously(19).

248

249 **Statistical analysis**

250 Data outliers were detected and eliminated using ROUT (robust regression and outlier analysis)
251 with Q set to 10%. Because our pilot experiments with a higher dose of Oxt (100 mcg/mL
252 concentration) showed no sex differences in the expression of oxidative stress markers in the
253 newborn brain, all subsequent analyses were performed regardless of sex of the offspring. RNA-
254 seq data were analyzed as described by us previously(19). Quantitative data were analyzed with
255 Welch's t-test with $p \leq 0.05$ considered significant, while oxidative stress gene expression data
256 were analyzed with unpaired student's t-test followed by Bonferroni correction with an adjusted
257 p-value ≤ 0.003 considered significant. All analyses, with the exception of RNA-seq data, were
258 performed on Prism 8 for Mac OS X (Graphpad Software, Inc, La Jolla, CA) and expressed as
259 mean \pm S.E.M.

260

261 **RESULTS**

262

263 **Development of the model for labor induction with Oxt**

264 Overall, 44 timed-pregnant Sprague Dawley dams were used for the study (Supplementary Table
265 S1). A video walkthrough of the experimental setup is presented as Supplementary Movie S1.
266 With the final regimen for Oxt as described in Methods, dams gave birth to pups predictably
267 within 8-12 h. Litter size and weight gain trajectory of the offspring from one experimental

268 cohort are presented in Supplementary Table S2. Handling of critical steps and troubleshooting
269 are described in greater detail in the Supplementary Materials and Methods.

270

271 **Validation of the model**

272 The best validation of our model was the successful vaginal delivery of thriving pups within 12 h
273 after initiation of the Oxt regimen (Supplementary Movie S2). In addition, we confirmed the
274 presence of immunoreactive phosphorylated myosin light chain kinase (MLCK)(29), a
275 serine/threonine kinase and a downstream regulator of the effects of Oxt on the actin-myosin
276 ATPase, in Oxt-exposed myometrium (**Fig. 4A**). Next, we confirmed that Oxt initiation was
277 accompanied by a rise in intrauterine pressure, a *sine qua non* feature of labor(30-32), and lasting
278 until birth of all pups (**Fig. 4B**). This was associated with an increase in OxtR gene expression in
279 the uterine myometrium (**Fig. 4C**). In contrast, exposure to Oxt for at least 8 h resulted in a
280 decrease in OxtR immunoreactivity (**Fig. 4D**) and membrane bound OxtR protein expression
281 (**Fig. 4E**) similar to human data. Collectively, we established the translational relevance of our
282 model by mirroring both Oxt management of labor and its effect on the uterine myometrium.

283

284 **Effect of surgery and anesthesia during pump implantation on the developing brain**

285 Because exposure to anesthesia and surgery can affect the developing brain(22, 23, 33-35), we
286 compared the cortical transcriptomes of newborn pups born to spontaneously laboring dams that
287 were not exposed to pump implantation surgery *vs.* those that were implanted with a saline-filled

288 pump on E18 (and therefore requiring anesthesia). Unbiased RNA-seq analyses of the cerebral
289 cortex of vaginally delivered newborn pups revealed no significant changes in the cortical
290 transcriptome after exposure to surgery and anesthesia as shown by the lack of significantly
291 differentially expressed genes in the volcano plot (**Fig. 5A**; heat map in Supplementary Fig. S1.).
292 Principal component analysis (**Fig. 5B**) revealed that the major source of variance was not the
293 treatment condition but the sex of the offspring, albeit not significant. Top up- and
294 downregulated genes from GO and KEGG analyses are presented in **Fig. 5C-E**. A
295 comprehensive list of differentially expressed genes and unadjusted p-value significant
296 differentially expressed genes is provided in Supplementary Data S1 and S2, respectively.

297

298 **Examination of the redox state of the fetal cortex after labor induction with Oxt**

299 Labor induction with Oxt was not associated with changes in the concentration of total free
300 radicals, 4-hydroxynonenal or protein carbonyl, in the newborn cortex. Nor were there any
301 significant differences in antioxidant capacity; both glutathione and total antioxidant capacity
302 were unchanged after Oxt (**Fig. 6A**). Furthermore, we did not observe any significant changes in
303 the expression of emblematic genes pertinent to the oxidative stress/antioxidant pathway (**Fig.**
304 **6B**; TaqMan qPCR probe list in Supplementary Table S3). Collectively, these data provide
305 reassurance that the use of Oxt for labor induction is unlikely to be associated with oxidative
306 stress in the fetal brain.

307

308

309 **COMMENT**

310 **Principal Findings**

311 Here, we present a realistic and tractable animal model for labor induction with Oxt. In addition
312 to functional validation of the model, we were able to demonstrate features consistent with the
313 use of Oxt in human labor: (i) a decrease in OxtR protein expression in the uterine myometrium,
314 and (ii) confirmation of increased intrauterine pressure with Oxt. Furthermore, we provide
315 evidence for the translational utility of the model by showing that labor induction with Oxt was
316 not associated with oxidative stress in the fetal brain.

317

318 **Results in the Context of What is Known**

319 Regarding use of Oxt to induce birth, the only other relevant preclinical study is that of
320 Hirayama et al. which used an osmotic pump to deliver a continuous subcutaneous infusion of
321 Oxt in pregnant mice(36). However, the experimental paradigm did not allow for escalation of
322 Oxt dose nor assessment of the impact of Oxt administration on the uterine myometrium.
323 Another study examined the impact of intravenous Oxt infusion on the fetal brain response to
324 hypoxia/anoxia and showed that pre-conditioning with Oxt increased the concentration of lactate
325 in the fetal brain but reduced the level of malondialdehyde, a lipid peroxidation marker(17).
326 Nevertheless, this study was designed to study the effect of Oxt on the brain adaptation to
327 hypoxia and not to assess the impact of Oxt on the process of birthing. Furthermore, Oxt was
328 administered as a constant infusion, unlike the gradually escalating rate used in our study. These
329 differences perhaps explain why we did not observe a decrease in oxidative stress in the fetal
330 brain. As a G protein-coupled receptor that is sensitive to downregulation, our findings of
331 reduced membrane bound OxtR protein expression after Oxt exposure is broadly consistent with

332 published data in human studies(6). However, to our surprise, expression of the OxtR gene was
333 significantly increased after labor induction with Oxt. We believe that these apparently
334 contradictory findings could be due to the choice of myometrial samples by Phaneuf et al.(6);
335 samples were collected from patients who underwent cesarean delivery after dystocic labor with
336 Oxt suggesting the possibility of abnormal transcription during intrapartum arrest of labor. In
337 contrast, we performed cesarean delivery during uncomplicated labor to facilitate sample
338 collection. This line of thought is supported by the 4-5-fold increased myometrial expression of
339 OxtR gene during uncomplicated labor in rodents(37, 38).

340

341 **Clinical Implications**

342 Our findings were reassuring in that even after 8-12 h of exposure to Oxt-induced uterine
343 contractions, there was no evidence for oxidative stress in the newborn brain. Lack of oxidative
344 stress after prolonged exposure to repetitive Oxt-induced uterine contractions in a species in
345 which labor typically lasts between 90-120 min(39), gives us more confidence that this is
346 unlikely to be a concern for the human fetus. Because of the wide variability in Oxt use across
347 the world(40), future research should focus on altering the dose regimens to determine if some of
348 the clinical observations related to oxidative stress are due to differences in Oxt dosing.

349

350 **Research Implications**

351 Ethical and logistic challenges significantly limit the scope of mechanistic research on pregnant
352 women and their newborn. Our contextually relevant animal model, by providing unrivaled
353 access to maternal and fetal tissue, has wide-ranging implications for translational research
354 related to perinatal Oxt exposure. This makes our model well suited to investigate lingering

355 concerns about the impact of Oxt on neurobehavioral development of the offspring(8, 14, 41,
356 42), epigenetic regulation of OxtR in the fetal brain(18), relationship between intrapartum Oxt
357 use and breastfeeding success(43-45), and the complex association between Oxt and postpartum
358 depression(46-48). Furthermore, by scaling down with appropriate equipment (iPRECIO[®] SMP
359 310-R with a dedicated wireless communication device), transgenic mouse models could be used
360 to investigate complex gene-environment interaction studies in the perinatal period. Ongoing
361 studies in our laboratory are focused on the transfer of maternally administered Oxt across the
362 placental and fetal blood-brain barriers, and its impact on Oxt-ergic signaling in the fetal brain.
363 Because of the critical importance of Oxt-ergic signaling for satiety and appetite regulation(49),
364 we are also particularly interested in the impact of perinatal Oxt exposure on childhood obesity.

365

366 **Strengths and Limitations**

367 The biggest strength of our model is how it mirrors labor induction with Oxt in clinical practice.
368 We prefer not to anthropomorphize our study because biological validation of the effect of
369 oxytocin with the birth of living pups was our motivation. However, the cumulative Oxt dose
370 until birth of the pups, approximately 3-7 μg , is comparable to the dose ranges typically used
371 during human labor. For example, parturients receive on average, a cumulative Oxt dose of
372 2000-4000 mIU or 2-4 IU (IU = International Unit) during the course of labor (50). Because 1 IU
373 = 1.68 μg of Oxt peptide, this would translate to approximately 3.4-6.8 μg of Oxt, similar to what
374 we used in our model. Considering that our model simulates clinical practice to a large extent,
375 research knowledge generated using this model is more likely to provide reliable and actionable
376 mechanistic data than other currently available models.

377

378 Our research has a few limitations. First, our model can be perceived as contrived. Considering
379 the technical challenges of delivering an escalating dose of intravenous Oxt in a free-moving
380 animal to simulate obstetric practice, we considered all possibilities before pursuing this model.
381 Importantly, our model is in no way more traumatic or less realistic than the unilateral carotid
382 artery ligation/ anoxia model to investigate perinatal asphyxia in rodents (51, 52). Second, even
383 though our low-dose Oxt infusion for the first 4 h would have resulted in cervical ripening as
384 demonstrated in laboring women (53), we are unable to provide objective evidence to support
385 that assumption. Nevertheless, because birth of the pups occurred predictably, it is likely a moot
386 concern. Third, we did not compare the extent to which Oxt increases intrauterine pressure
387 compared to saline. Because we had biological validation of pup birth, our objective was to
388 capture the temporal relationship between the initiation of Oxt and the rise in intrauterine
389 pressure rather than assess differences in intrauterine pressure between Oxt-induced and
390 spontaneous labor that have been characterized previously(54).

391

392 **Conclusions**

393 In conclusion, we provide a viable and realistic animal model for labor induction and
394 augmentation with Oxt and demonstrate its utility in addressing clinically relevant questions in
395 obstetric practice. Adoption of our model by other researchers would enable new lines of
396 investigation related to the impact of perinatal Oxt exposure on the mother-infant dyad.

397

398

399

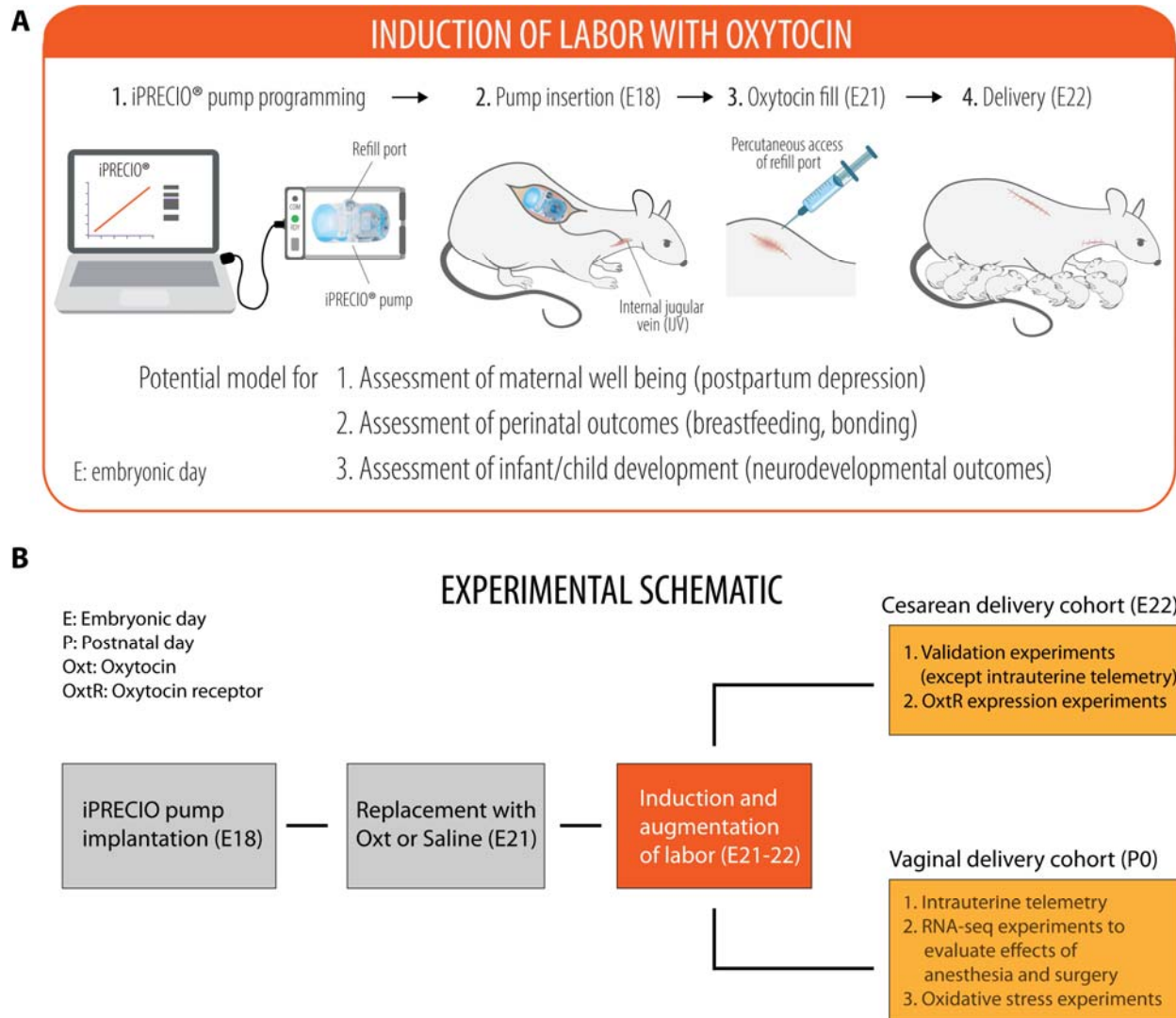
400

401 **Figures and Figure Legends**

402

403 **Figure 1**

404



405

406

407 **Fig. 1. Experimental schematic for labor induction with oxytocin in term pregnant rat. (A)**

408 A cartoon depicting the programming and implantation of iPRECIO® pump in a pregnant rat

409 followed by birth of healthy pups. (B) Experimental schematic showing the overall experimental

410 outline with two separate cohorts for cesarean and vaginal delivery. In the vaginal delivery
411 cohort, there were three sets of independent experiments for (i) intrauterine telemetry, (ii) RNA-
412 seq experiments to assess the impact of in utero exposure to anesthesia and surgery on the
413 cortical transcriptome of the newborn brain, and (iii) examination of oxidative stress in newborn
414 pups after either Oxt or saline, respectively.

415

416

417

418

419

420

421

422

423

424

425

426

427

428

429

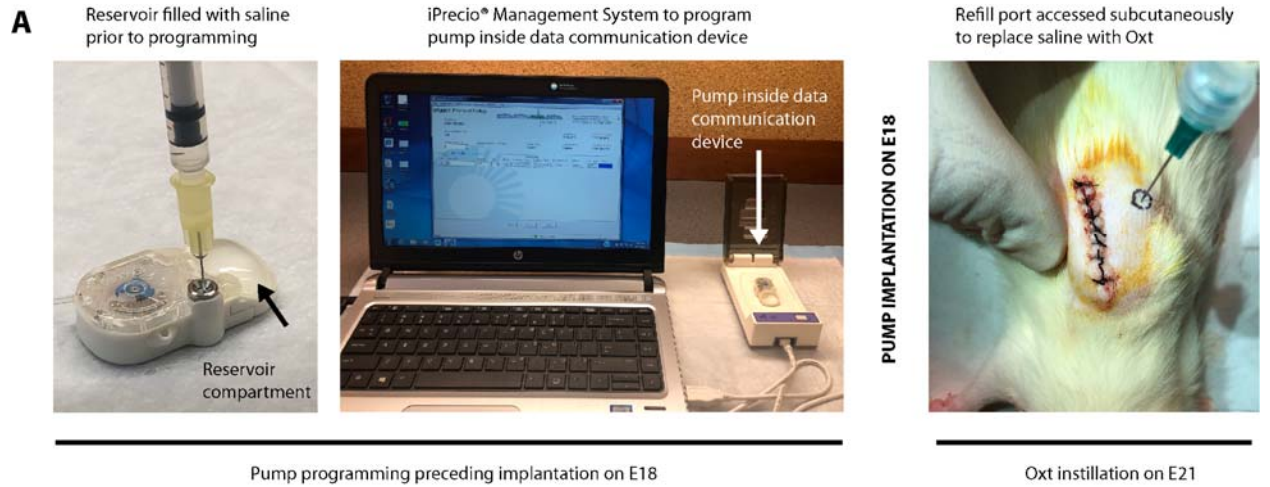
430

431

432

433 **Figure 2**

434



435

436

437 **Fig. 2. Workflow of experimental and surgical procedures associated with creation of the**
438 **model. (A)** Workflow for iPRECIO[®] pump programming prior to implantation on E18 and
439 subsequent replacement of saline with Oxt by subcutaneous access of the refill port on E21. **(B)**
440 Left to right: sequential surgical workflow for implantation of the pre-programmed iPRECIO[®]
441 pump followed by internal jugular vein cannulation with the pump catheter on E18. All surgical
442 procedures were performed in strict accordance with institutional guidelines for rodent surgery,
443 anesthesia, and analgesia.

444

445

446

447

448

449

450

451

452

453

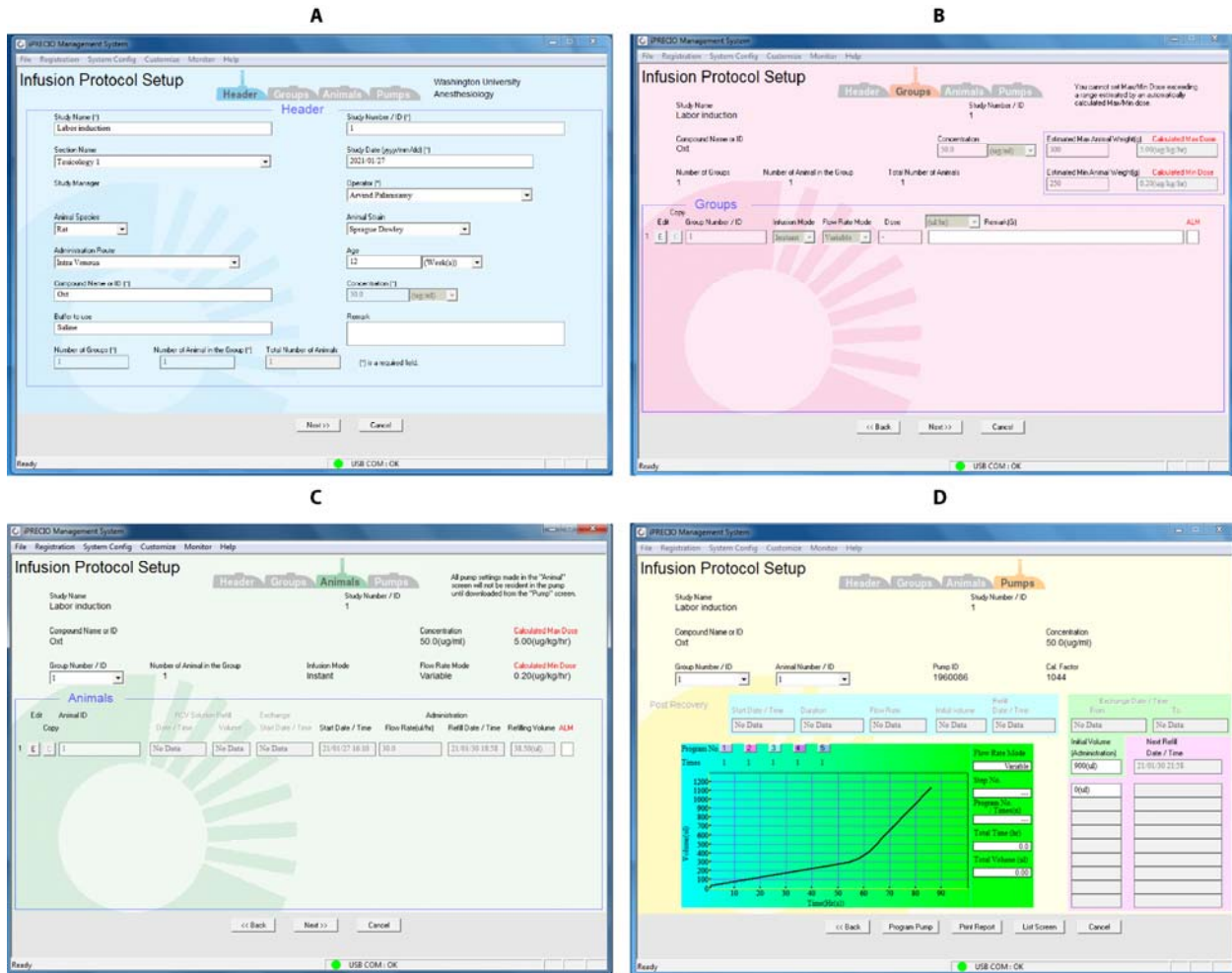
454

455

456

457

458 **Figure 3**



459

460

461 **Fig. 3. A walkthrough of the sequential steps (A-D) for pump programming with**

462 **iPRECIO[®] Management System software.** All procedures were performed in accordance with

463 the manufacturer's instructions. **(A)** Infusion protocol set up page that allows input of all the

464 variables necessary for programming of the pump. **(B-C)** Variable flow rate mode is chosen to

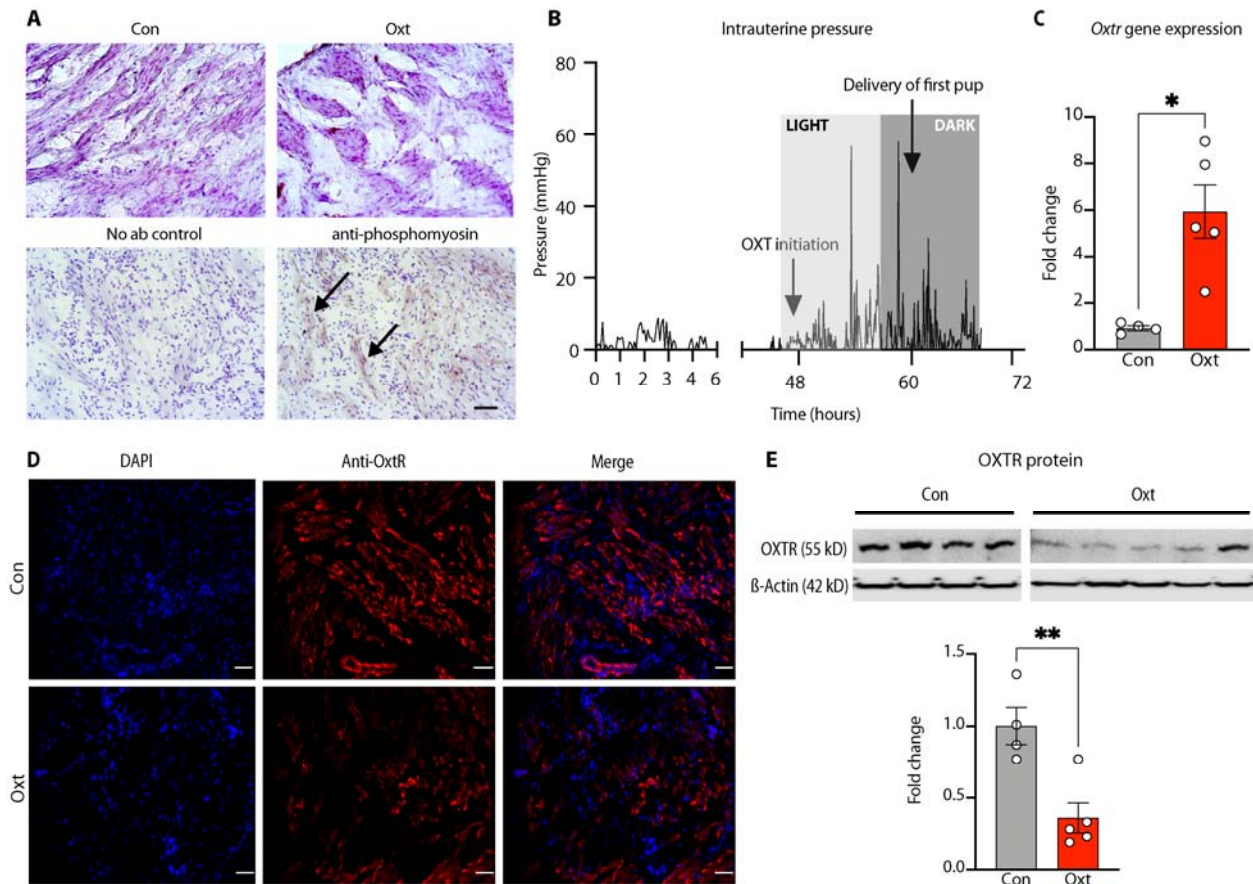
465 ensure gradual escalation of Oxt dose over time. **(D)** A graphic representation of Oxt dosing

466 showing the volume that is to be administered over time. The pump ID and calibration factor is

467 automatically detected and inputted by the data communication device.

468 **Figure 4**

469



470

471

472 **Fig. 4. Validation of the model for labor induction with oxytocin.** (A) Visualization of uterine
473 contraction. Upper panel: uterine myometrium harvested from pregnant E21 rats at least 8 h after
474 either saline (control) or intravenous Oxt infusion and stained with hematoxylin. 20x
475 photomicrographs showing lack of clustering of uterine myocytes in saline-treated myometrium
476 (left) compared to extensive clustering in the Oxt-exposed myometrium (right). Lower panel: 5-
477 μ m frozen sections from Oxt-exposed myometrium stained without (left) or with rabbit anti-
478 mouse phosphomyosin light chain kinase showing prominent staining among clustered uterine
479 myocytes revealed with anti-rabbit HRP conjugate (marked by arrows) (right). Nuclei

480 counterstained with hematoxylin. Scale bar = 100 μ M. **(B)** Labor induction with Oxt causes
481 cyclical increases in intrauterine pressure. Labor was induced with Oxt at 48 h after pump
482 implantation (around 12 noon, light cycle, E20) and intrauterine pressure changes were
483 monitored with telemetry. Oxt initiation was associated with acute and cyclical increases in
484 intrauterine pressure until birth (first pup delivered around 21:00 h, dark cycle, E20). Light and
485 dark cycle from 07:00-19:00 and 19:00-07:00, respectively. **(C)** Labor induction with Oxt was
486 associated with a significant increase in OxtR gene expression at 8-12 h. **(D)** Labor induction
487 with Oxt decreases OxtR immunoreactivity in the rat uterus. Sample 20x photomicrographs from
488 5- μ m sections of the uterine myometrium stained with goat anti-rat OxtR antibody (1:100) and
489 revealed with Alexa Fluor[®] 594 labeled rabbit anti-goat antibody (1:300). Note naïve uterine
490 myometrium with bright staining for OxtR in the upper panel, in sharp contrast to Oxt-exposed
491 myometrial tissue in the lower panel where staining was scant, suggesting downregulation of
492 OxtR. Scale bar = 50 μ M. **(E)** Representative western blot showing a decrease in membrane
493 associated OxtR protein expression after labor induction with Oxt and quantified with
494 densitometry. Data analyzed with Welch's t-test and presented as mean \pm SEM; * $p \leq 0.05$, ** $p \leq$
495 0.01.

496

497

498

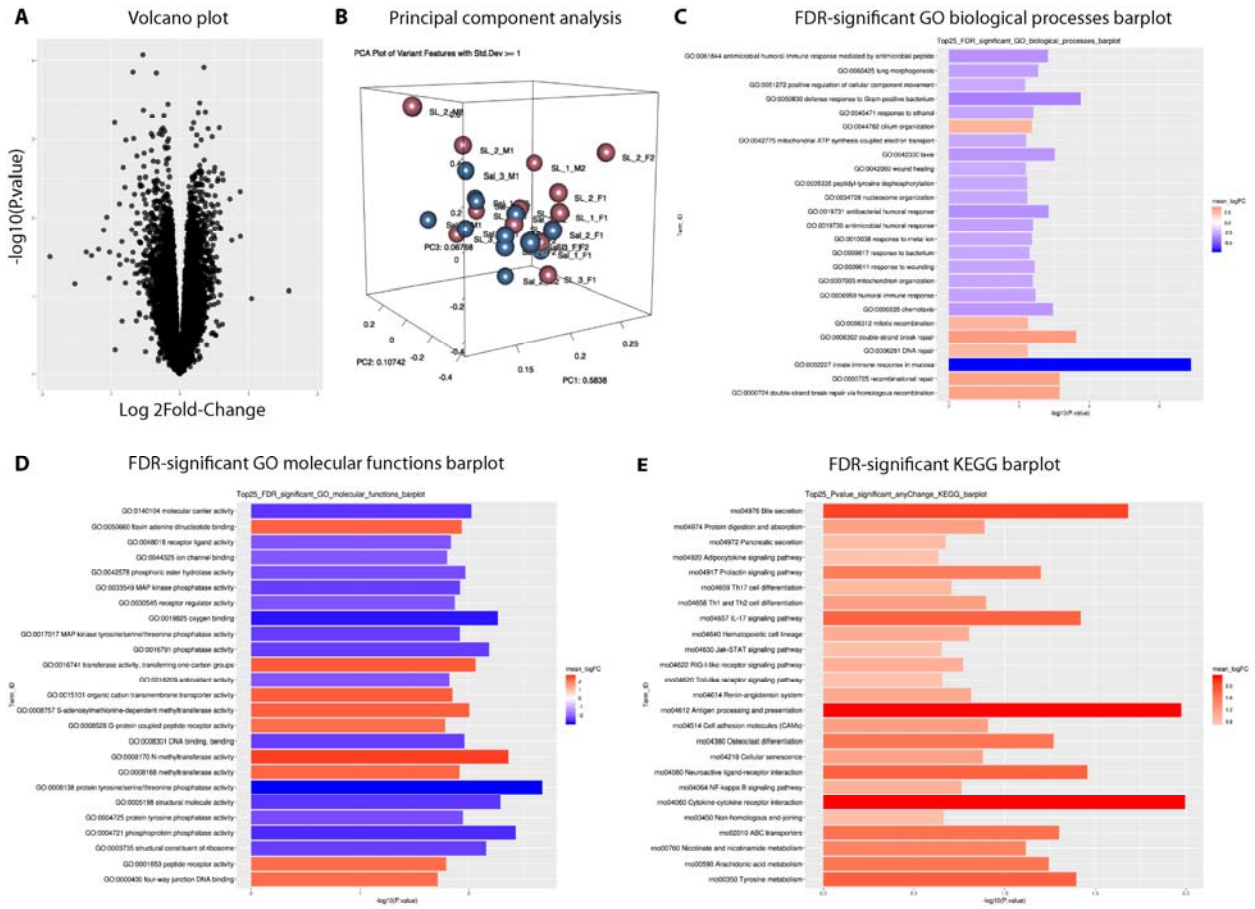
499

500

501

502 **Figure 5**

503



504

505 **Fig. 5. Impact of anesthesia and surgery on the newborn cortical transcriptome. (A)**
 506 Volcano plot showing the absence of significantly differentially expressed genes between the
 507 spontaneous labor vs. saline pump groups (n = 2 pups of each sex/dam from 3 dams/treatment
 508 condition). **(B)** Principal component analysis (PCA) showing that the major source of variance is
 509 not the treatment condition (fuchsia: spontaneous labor, blue: saline pump) but the sex of the
 510 offspring, albeit not significant. **(C-D)** Top 25 false discovery rate-adjusted significantly up- and
 511 downregulated genes for Gene Ontology (GO) biological processes (C) and molecular functions
 512 (D) after labor induction with Oxt. **(E)** Significantly upregulated genes with Kyoto Encyclopedia

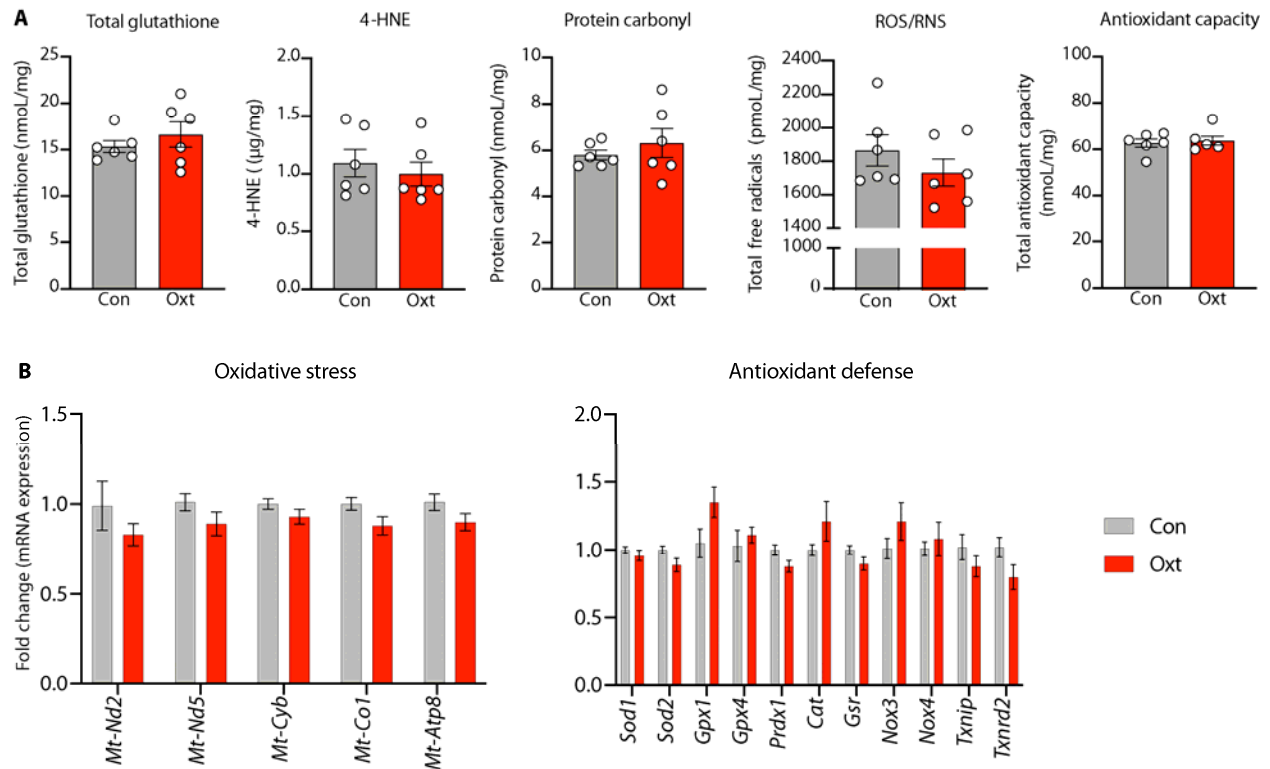
513 of Genes and Genomes (KEGG) analysis. GO and KEGG analyses revealed a differential impact
514 of anesthesia and surgery on multiple pathways, mostly related to oxygen binding and the
515 immune response, respectively. Therefore, for the rest of our experiments, we used saline pump-
516 implanted dams that eventually labored spontaneously as controls, instead of dams that labored
517 spontaneously without exposure to anesthesia and surgery.

518

519

520 **Figure 6**

521



522

523

524 **Fig. 6. Labor induction with oxytocin is not associated with oxidative stress in the**
525 **developing brain. (A)** From left to right: Labor induction with oxytocin was not associated with
526 an increase in either glutathione, 4-hydroxynonenal, protein carbonyl, reactive oxygen/nitrogen
527 species (ROS/RNS), or total antioxidant capacity in the developing fetal cortex. All data are
528 presented per mg of brain protein. **(B)** Expression of genes mediating oxidative stress or
529 antioxidant defense were not significantly differentially expressed in the fetal cortex after labor
530 induction with oxytocin. Collectively, these data indicate that labor induction with Oxt is
531 unlikely to be associated with oxidative stress in the developing brain. Data were analyzed with
532 Welch's t-test and expressed as mean \pm SEM (n=5-8 per treatment condition with pups
533 represented from all unique dams).

534 **References**

535

536 1. Obstetrics ACoPB--. ACOG Practice Bulletin No. 107: Induction of labor. *Obstet*
537 *Gynecol.* 2009;114(2 Pt 1):386-97.

538 2. Osterman MJ, Martin JA. Recent declines in induction of labor by gestational age. *NCHS*
539 *Data Brief.* 2014(155):1-8.

540 3. Martin JA, Hamilton BE, Osterman MJK, Driscoll AK, Drake P. Births: Final Data for
541 2016. *Natl Vital Stat Rep.* 2018;67(1):1-55.

542 4. Grobman WA, Rice MM, Reddy UM, Tita ATN, Silver RM, Mallett G, et al. Labor
543 Induction versus Expectant Management in Low-Risk Nulliparous Women. *N Engl J Med.*
544 2018;379(6):513-23.

545 5. Souter V, Painter I, Sitcov K, Caughey AB. Maternal and newborn outcomes with
546 elective induction of labor at term. *Am J Obstet Gynecol.* 2019;220(3):273 e1- e11.

547 6. Phaneuf S, Rodriguez Linares B, TambyRaja RL, MacKenzie IZ, Lopez Bernal A. Loss
548 of myometrial oxytocin receptors during oxytocin-induced and oxytocin-augmented labour. *J*
549 *Reprod Fertil.* 2000;120(1):91-7.

550 7. Crane JM, Young DC, Butt KD, Bennett KA, Hutchens D. Excessive uterine activity
551 accompanying induced labor. *Obstet Gynecol.* 2001;97(6):926-31.

552 8. Gregory SG, Anthopolos R, Osgood CE, Grotegut CA, Miranda ML. Association of
553 autism with induced or augmented childbirth in North Carolina Birth Record (1990-1998) and
554 Education Research (1997-2007) databases. *JAMA Pediatr.* 2013;167(10):959-66.

555 9. Weisman O, Agerbo E, Carter CS, Harris JC, Uldbjerg N, Henriksen TB, et al. Oxytocin-
556 augmented labor and risk for autism in males. *Behav Brain Res.* 2015;284:207-12.

- 557 10. Friedlander E, Feldstein O, Mankuta D, Yaari M, Harel-Gadassi A, Ebstein RP, et al.
558 Social impairments among children perinatally exposed to oxytocin or oxytocin receptor
559 antagonist. *Early Hum Dev.* 2017;106-107:13-8.
- 560 11. Kurth L, Haussmann R. Perinatal Pitocin as an early ADHD biomarker:
561 neurodevelopmental risk? *J Atten Disord.* 2011;15(5):423-31.
- 562 12. Guastella AJ, Cooper MN, White CRH, White MK, Pennell CE, Whitehouse AJO. Does
563 perinatal exposure to exogenous oxytocin influence child behavioural problems and autistic-like
564 behaviours to 20 years of age? *J Child Psychol Psychiatry.* 2018;59(12):1323-32.
- 565 13. Oberg AS, D'Onofrio BM, Rickert ME, Hernandez-Diaz S, Ecker JL, Almqvist C, et al.
566 Association of Labor Induction With Offspring Risk of Autism Spectrum Disorders. *JAMA*
567 *Pediatr.* 2016;170(9):e160965.
- 568 14. Soltys SM, Scherbel JR, Kurian JR, Diebold T, Wilson T, Hedden L, et al. An association
569 of intrapartum synthetic oxytocin dosing and the odds of developing autism. *Autism.*
570 2020;24(6):1400-10.
- 571 15. Boer GJ. Chronic oxytocin treatment during late gestation and lactation impairs
572 development of rat offspring. *Neurotoxicol Teratol.* 1993;15(6):383-9.
- 573 16. Boer GJ, Kruisbrink J. Effects of continuous administration of oxytocin by an accurel
574 device on parturition in the rat and on development and diuresis in the offspring. *J Endocrinol.*
575 1984;101(2):121-9.
- 576 17. Boksa P, Zhang Y, Nouel D. Maternal Oxytocin Administration Before Birth Influences
577 the Effects of Birth Anoxia on the Neonatal Rat Brain. *Neurochem Res.* 2015;40(8):1631-43.

- 578 18. Kenkel WM, Perkeybile AM, Yee JR, Pournajafi-Nazarloo H, Lillard TS, Ferguson EF,
579 et al. Behavioral and epigenetic consequences of oxytocin treatment at birth. *Sci Adv.*
580 2019;5(5):eaav2244.
- 581 19. Palanisamy A, Giri T, Jiang J, Bice A, Quirk JD, Conyers SB, et al. In utero exposure to
582 transient ischemia-hypoxemia promotes long-term neurodevelopmental abnormalities in male rat
583 offspring. *JCI Insight.* 2020;5(10).
- 584 20. Pierce SL, Kutschke W, Cabeza R, England SK. In vivo measurement of intrauterine
585 pressure by telemetry: a new approach for studying parturition in mouse models. *Physiol*
586 *Genomics.* 2010;42(2):310-6.
- 587 21. Rada CC, Pierce SL, Grotegut CA, England SK. Intrauterine telemetry to measure mouse
588 contractile pressure in vivo. *Journal of visualized experiments : JoVE.* 2015(98):e52541.
- 589 22. Palanisamy A. Maternal anesthesia and fetal neurodevelopment. *Int J Obstet Anesth.*
590 2012;21(2):152-62.
- 591 23. Palanisamy A, Baxter MG, Keel PK, Xie Z, Crosby G, Culley DJ. Rats exposed to
592 isoflurane in utero during early gestation are behaviorally abnormal as adults. *Anesthesiology.*
593 2011;114(3):521-8.
- 594 24. Calderon TC, Wu W, Rawson RA, Sakala EP, Sowers LC, Boskovic DS, et al. Effect of
595 mode of birth on purine and malondialdehyde in umbilical arterial plasma in normal term
596 newborns. *J Perinatol.* 2008;28(7):475-81.
- 597 25. Schneid-Kofman N, Silberstein T, Saphier O, Shai I, Tavor D, Burg A. Labor
598 augmentation with oxytocin decreases glutathione level. *Obstet Gynecol Int.* 2009;2009:807659.

- 599 26. Murphy M, Butler M, Coughlan B, Brennan D, O'Herlihy C, Robson M. Elevated
600 amniotic fluid lactate predicts labor disorders and cesarean delivery in nulliparous women at
601 term. *Am J Obstet Gynecol.* 2015;213(5):673 e1-8.
- 602 27. Wiberg-Itzel E, Pembe AB, Wray S, Wihlback AC, Darj E, Hoesli I, et al. Level of
603 lactate in amniotic fluid and its relation to the use of oxytocin and adverse neonatal outcome.
604 *Acta Obstet Gynecol Scand.* 2014;93(1):80-5.
- 605 28. Perrone S, Tataranno LM, Stazzoni G, Ramenghi L, Buonocore G. Brain susceptibility to
606 oxidative stress in the perinatal period. *J Matern Fetal Neonatal Med.* 2015;28 Suppl 1:2291-5.
- 607 29. Moore F, Bernal AL. Myosin light chain kinase and the onset of labour in humans. *Exp*
608 *Physiol.* 2001;86(2):313-8.
- 609 30. Seitchik J, Chatkoff ML. Intrauterine pressure wave form characteristics in
610 hypocontractile labor before and after oxytocin administration. *Am J Obstet Gynecol.*
611 1975;123(4):426-34.
- 612 31. Seitchik J, Chatkoff ML. Oxytocin-induced uterine hypercontractility pressure wave
613 forms. *Obstetrics and gynecology.* 1976;48(4):436-41.
- 614 32. Bakker PC, Van Rijswijk S, van Geijn HP. Uterine activity monitoring during labor. *J*
615 *Perinat Med.* 2007;35(6):468-77.
- 616 33. Adhikari A. Distributed circuits underlying anxiety. *Front Behav Neurosci.* 2014;8:112.
- 617 34. Creeley CE, Dikranian KT, Dissen GA, Back SA, Olney JW, Brambrink AM. Isoflurane-
618 induced apoptosis of neurons and oligodendrocytes in the fetal rhesus macaque brain.
619 *Anesthesiology.* 2014;120(3):626-38.
- 620 35. Vutskits L, Xie Z. Lasting impact of general anaesthesia on the brain: mechanisms and
621 relevance. *Nat Rev Neurosci.* 2016;17(11):705-17.

- 622 36. Hirayama T, Hiraoka Y, Kitamura E, Miyazaki S, Horie K, Fukuda T, et al. Oxytocin
623 induced labor causes region and sex-specific transient oligodendrocyte cell death in neonatal
624 mouse brain. *J Obstet Gynaecol Res.* 2020;46(1):66-78.
- 625 37. Helguera G, Eghbali M, Sforza D, Minosyan TY, Toro L, Stefani E. Changes in global
626 gene expression in rat myometrium in transition from late pregnancy to parturition. *Physiol*
627 *Genomics.* 2009;36(2):89-97.
- 628 38. Shchuka VM, Abatti LE, Hou H, Khader N, Dorogin A, Wilson MD, et al. The pregnant
629 myometrium is epigenetically activated at contractility-driving gene loci prior to the onset of
630 labor in mice. *PLoS Biol.* 2020;18(7):e3000710.
- 631 39. Catheline G, Touquet B, Besson JM, Lombard MC. Parturition in the rat: a physiological
632 pain model. *Anesthesiology.* 2006;104(6):1257-65.
- 633 40. Daly D, Minnie KCS, Blignaut A, Blix E, Vika Nilsen AB, Dencker A, et al. How much
634 synthetic oxytocin is infused during labour? A review and analysis of regimens used in 12
635 countries. *PLoS One.* 2020;15(7):e0227941.
- 636 41. Gottlieb MM. A Mathematical Model Relating Pitocin Use during Labor with Offspring
637 Autism Development in terms of Oxytocin Receptor Desensitization in the Fetal Brain. *Comput*
638 *Math Methods Med.* 2019;2019:8276715.
- 639 42. Wahl RU. Could oxytocin administration during labor contribute to autism and related
640 behavioral disorders?--A look at the literature. *Med Hypotheses.* 2004;63(3):456-60.
- 641 43. Jonas W, Johansson LM, Nissen E, Ejdeback M, Ransjo-Arvidson AB, Uvnas-Moberg K.
642 Effects of intrapartum oxytocin administration and epidural analgesia on the concentration of
643 plasma oxytocin and prolactin, in response to suckling during the second day postpartum.
644 *Breastfeed Med.* 2009;4(2):71-82.

- 645 44. Lara-Cinisomo S, McKenney K, Di Florio A, Meltzer-Brody S. Associations Between
646 Postpartum Depression, Breastfeeding, and Oxytocin Levels in Latina Mothers. *Breastfeed Med.*
647 2017;12(7):436-42.
- 648 45. Uvnas Moberg K, Ekstrom-Bergstrom A, Buckley S, Massarotti C, Pajalic Z, Luegmair
649 K, et al. Maternal plasma levels of oxytocin during breastfeeding-A systematic review. *PLoS*
650 *One.* 2020;15(8):e0235806.
- 651 46. Jobst A, Krause D, Maiwald C, Hartl K, Myint AM, Kastner R, et al. Oxytocin course
652 over pregnancy and postpartum period and the association with postpartum depressive
653 symptoms. *Arch Womens Ment Health.* 2016;19(4):571-9.
- 654 47. Kroll-Desrosiers AR, Nephew BC, Babb JA, Guilarte-Walker Y, Moore Simas TA,
655 Deligiannidis KM. Association of peripartum synthetic oxytocin administration and depressive
656 and anxiety disorders within the first postpartum year. *Depress Anxiety.* 2017;34(2):137-46.
- 657 48. Thul TA, Corwin EJ, Carlson NS, Brennan PA, Young LJ. Oxytocin and postpartum
658 depression: A systematic review. *Psychoneuroendocrinology.* 2020;120:104793.
- 659 49. Lawson EA. The effects of oxytocin on eating behaviour and metabolism in humans. *Nat*
660 *Rev Endocrinol.* 2017;13(12):700-9.
- 661 50. Roloff K, Peng S, Sanchez-Ramos L, Valenzuela GJ. Cumulative oxytocin dose during
662 induction of labor according to maternal body mass index. *Int J Gynaecol Obstet.*
663 2015;131(1):54-8.
- 664 51. Vannucci RC, Connor JR, Mauger DT, Palmer C, Smith MB, Towfighi J, et al. Rat
665 model of perinatal hypoxic-ischemic brain damage. *J Neurosci Res.* 1999;55(2):158-63.
- 666 52. Rumajogee P, Bregman T, Miller SP, Yager JY, Fehlings MG. Rodent Hypoxia-Ischemia
667 Models for Cerebral Palsy Research: A Systematic Review. *Front Neurol.* 2016;7:57.

668 53. Ferguson JE, 2nd, Head BH, Frank FH, Frank ML, Singer JS, Stefos T, et al. Misoprostol
669 versus low-dose oxytocin for cervical ripening: a prospective, randomized, double-masked trial.
670 Am J Obstet Gynecol. 2002;187(2):273-9; discussion 9-80.

671 54. Seitchik J, Chatkoff ML, Hayashi RH. Intrauterine pressure waveform characteristics of
672 spontaneous and oxytocin- or prostaglandin F₂α--induced active labor. Am J Obstet
673 Gynecol. 1977;127(3):223-7.

674

675

676

677

678

679

680

681

682

683

684

685

686

687

688

689

690

691 **Acknowledgments:** None.

692

693 **Author contributions**

694

695 Arvind Palanisamy: Conceptualization, Investigation, Methodology, Project Administration,

696 Resources, Software, Data Curation, Formal analysis, Supervision, Visualization, Writing

697 Tusar Giri: Investigation (model creation, molecular biology experiments), Methodology,

698 Validation, Writing

699 Jia Jiang: Investigation (model creation)

700 Zhiqiang Xu: Investigation (immunohistochemistry experiments)

701 Ron McCarthy: Investigation (intrauterine telemeter placement)

702 Carmen M. Halabi: Funding acquisition, Resources (telemetry monitoring), Writing

703 Sarah K. England: Funding acquisition, Methodology, Resources, Writing

704 Eric Tycksen: Data curation, Software, Formal analysis (RNA-seq data), Visualization, Writing

705 Alison G. Cahill. Writing – original draft, review & editing.

706

707 **Data sharing statement**

708

709 The equipment needed to establish the model are commercially available and non-proprietary.

710 All data needed to evaluate the conclusions in the paper are present in the paper and/or the

711 Supplementary Materials. The RNA-seq data used in this publication have been deposited in
712 NCBI's Gene Expression Omnibus (GEO) and are accessible through the GEO Series accession
713 number GSE161122 (<https://www.ncbi.nlm.nih.gov/geo/query/acc.cgi?acc=GSE161122>).

714

715

716

717

718

719

720

721

722

723

724

725

726

727

728

729

730

731 **Supplementary Files**

732

733 **1. Supplementary Materials and Methods**

734

735 **2. Supplementary Figures**

736

737 **Fig. S1.** RNA-seq data showing the heatmap of differentially expressed genes after *in utero*

738 exposure to anesthesia and surgery for pump implantation.

739

740 **3. Supplementary Tables**

741

742 **Table S1.** Animal use data.

743 **Table S2.** Litter data and weight gain trajectory of the offspring.

744 **Table S3.** Taqman qPCR probe list from ThermoFisher Scientific, Inc.

745

746 **4. Supplementary Movies**

747

748 **Movie S1.** Experimental set up for iPRECIO[®] pump implantation. A video walk-through of the

749 overall surgical set up for performing the experiments.

750 **Movie S2.** Appropriate and nurturing care of the newborn after low dose (50 mcg/mL) Oxt
751 regimen.

752 **Movie S3.** Poor maternal self-care and pup neglect in a dam implanted with iPRECIO[®] pump at
753 E20 and treated with high dose of Oxt (100 mcg/mL).

754

755 **5. Supplementary Data Files**

756

757 **Data S1.** RNA-seq data showing the list of significantly expressed genes in the developing
758 cortex after *in utero* exposure to anesthesia and surgery.

759

760 **Data S2.** RNA-seq data showing the list of false discovery rate-unadjusted significantly
761 expressed genes in the developing cortex after *in utero* exposure to anesthesia and surgery.

762

763

764

765

766

767

768

769

770

771

772

773

774

775